

PORE ALIGNMENT BETWEEN TWO DISSIMILAR SATURATED POROELASTIC MEDIA: REFLECTION AND REFRACTION AT THE INTERFACE

M. D. SHARMA and TRIBHAWAN SAINI

Department of Mathematics, Kurukshetra University, Kurukshetra-132 119, India

(Received 13 March 1991; in revised form 3 October 1991)

Abstract—Biot's theory is employed to study the reflection and refraction of plane harmonic waves at the welded interface between two dissimilar saturated poroelastic media. A pore alignment parameter is defined to classify the effects of connection between the interstices of the two media.

Effects of pore alignment on the amplitude ratios and energy ratios have been calculated numerically, for a particular model. Amplitude and energy ratios do not change significantly as we move from partial alignment to full alignment of pores. However, the effect on amplitudes and energies is quite significant for the values of the pore alignment parameter approaching zero. For extreme values of the pore alignment parameter, the amplitude and energy ratios have been plotted against the angle of incidence.

INTRODUCTION

Propagation of elastic waves in fluid-saturated porous media has been a subject of continued interest due to its importance in various fields, such as earthquake engineering, soil dynamics, foundation engineering, seismology, geophysics and hydrology. Biot (1956a, b) formulated the constitutive equations and equations of motion for such solids. He demonstrated the existence of two kinds of compressional waves along with one shear wave. Deresiewicz and Rice (1962) studied the reflection of plane waves at the free plane boundary of saturated poroelastic solids. The boundary conditions appropriate for the boundaries of such solids have been discussed by Deresiewicz and Skalak (1963). Burrige and Vargas (1979) justified the validity of constitutive equations derived by Biot in the study of seismic waves propagating in the earth. In recent years a number of problems regarding wave propagation at poroelastic solid interface have been studied, e.g. Hajra and Mukhopadhyay (1982), Yew and Wang (1987), Sharma *et al.* (1990a, b). In all these studies, poroelastic solids are assumed to be in contact with a liquid or an impervious elastic solid. Not much work has been done for the wave propagation at a poroelastic/poroelastic interface. At such an interface, boundary conditions depend upon the connection between the interstices of the two media in contact.

In the present study, reflection and refraction at the interface between two different saturated poroelastic media has been discussed. Effects of connection between the interstices of the two media on the amplitude and energy ratios have been exhibited for a particular model.

FIELD EQUATIONS

Following Biot (1962), the differential equations governing the displacement \hat{u} of solid matrix and \hat{U} of interstitial fluid in a homogeneous poroelastic solid, in the absence of dissipation, are

$$\begin{aligned} \mu \nabla^2 \hat{u} + (\lambda + \mu + \alpha^2 M) \text{grad} (\nabla \cdot \hat{u}) + \alpha M \text{grad} (\nabla \cdot \hat{w}) \\ = \partial^2 (\rho \hat{u} + \rho_f \hat{w}) / \partial t^2 \text{grad} \{ \alpha M (\nabla \cdot \hat{u}) + M (\nabla \cdot \hat{w}) \} = \partial^2 (\rho_s \hat{u} + m \hat{w}) / \partial t^2. \quad (1) \end{aligned}$$

The vector \hat{w} , $\{ = \beta (\hat{U} - \hat{u}) \}$, represents the flow of fluid relative to the solid measured per unit area of the bulk medium, $\lambda, \mu =$ Lamé's constants for the solid, $\rho, \rho_f =$ mass densities of the bulk material and fluid respectively, $m =$ Biot's parameter which depends upon

porosity β and ρ_f , and α and M are elastic constants related to coefficients of jacketed and unjacketed compressibilities.

The stress components in the solid, T_{ij} , and fluid pressure p_f are expressed as

$$\begin{aligned} T_{ij} &= 2\mu e_{ij} + \{(\lambda + \alpha^2 M)e + \alpha M \xi\} \delta_{ij}, \quad (i, j = 1, 2, 3) \\ p_f &= -M\{\alpha e + \xi\} \end{aligned} \quad (2)$$

where $e = \text{div } \bar{u}$, $\xi = \text{div } \bar{w}$ and

$$e_{ij} = \frac{1}{2}\{u_{i,j} + u_{j,i}\}. \quad (3)$$

Following Sharma and Gogna (1991), the displacements \bar{u} and \bar{w} can be expressed as

$$\begin{aligned} \bar{u} &= \text{grad } \phi_1 + \text{grad } \phi_2 + \text{curl } \Psi_1, \\ \bar{w} &= \mu_1 \text{grad } \phi_1 + \mu_2 \text{grad } \phi_2 + \alpha_0 \text{curl } \Psi_1, \end{aligned} \quad (4)$$

where

$$\mu_j = (\rho_f \alpha - \rho + \rho_j)/(\rho_f - m\alpha), \quad (j = 1, 2). \quad (5)$$

The mass densities ρ_j ($j = 1, 2, 3$) are given by

$$\rho_j = \{B + (-1)^j \sqrt{(B^2 - 4AC)}\}/2M, \quad (j = 1, 2); \rho_3 = C/M, \quad (6)$$

where

$$A = (\lambda + 2\mu)M, \quad B = \rho M + mH - 2\rho_f \alpha M, \quad C = \rho m - \rho^2, \quad H = \lambda + 2\mu + \alpha^2 M. \quad (7)$$

Potentials ϕ_1 , ϕ_2 and Ψ_1 satisfy the wave equations, i.e.

$$(\nabla^2 + \delta_j^2)\phi_j = 0, \quad (j = 1, 2); (\nabla^2 + \delta_3^2)\Psi_1 = 0, \quad (8)$$

where

$$\delta_j^2 = \Omega^2/v_j^2, \quad (j = 1, 2, 3). \quad (9)$$

Ω is angular frequency and velocities of propagation, v_j ($j = 1, 2, 3$), are given by

$$v_j^2 = (\lambda + 2\mu)/\rho_j, \quad (j = 1, 2); v_3^2 = \mu/\rho_3. \quad (10)$$

The wave corresponding to ϕ_1 is called fast P (or P_f) wave; the wave corresponding to ϕ_2 is called slow P (or P_s) wave and that corresponding to the vector potential Ψ_1 is the only shear wave.

FORMULATION OF THE PROBLEM

We consider two different homogeneous isotropic fluid-saturated porous solids in welded contact along a plane interface. Rectangular Cartesian coordinate system (x, y, z) is chosen with plane of interface as $z = 0$ and z -axis pointing into the medium M' , as shown in Fig. 1. The medium M through which incidence takes place occupies the region $z < 0$ and the region $z > 0$ is occupied by the medium M' . Considering the two-dimensional reflection-refraction problem, we shall restrict the plane wave solutions in the plane perpendicular to the interface.

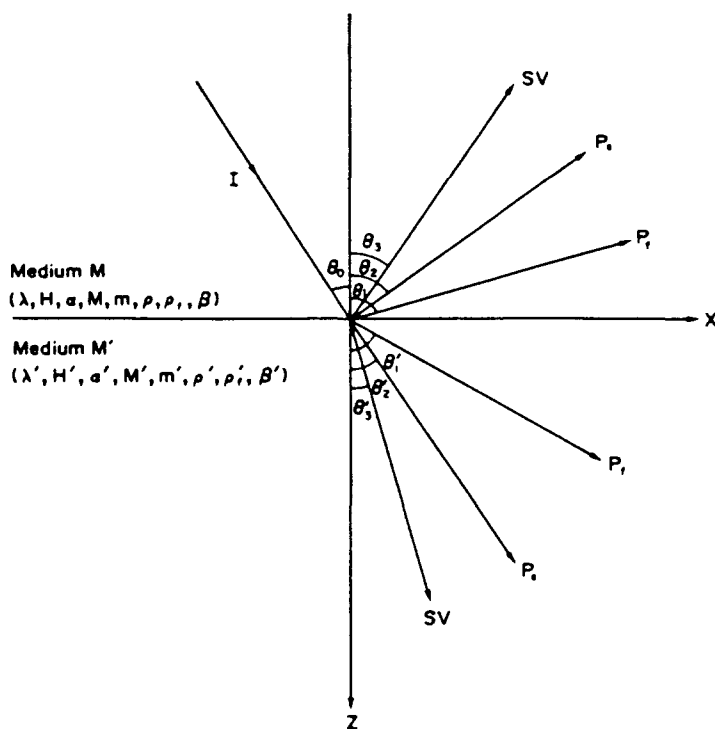


Fig. 1. Geometry of the problem.

BOUNDARY CONDITIONS

Following Deresiewicz and Skalak (1963), nonalignment of a portion of the pores can produce an interfacial flow area which is smaller than that in either medium adjacent to the interface. If we define $\beta_0 = \min(\beta, \beta')$ and $\epsilon\beta_0$ ($0 \leq \epsilon \leq 1$) as the interfacial flow area in the interface element of unit area then ϵ is assumed as pore alignment parameter. $\epsilon = 1$ implies that pores of two media are completely connected at the interface and $\epsilon = 0$ corresponds to the case when there is no connection between the interstices of two media. The effect of nonalignment of the portion of pores might be accomplished physically by inserting a porous membrane between the two poroelastic media with fully aligned pores. Flow through such an interface would result in a pressure drop across the interface. As the pores in each of the individual poroelastic media are assumed to be interconnected, we assume that even the alignment of a small portion of the pores would result in the large reduction in the pressure drop, at the interface. Therefore, with the assumed consistency between the pressure drop and normal component of filtration velocity, we choose to write the continuity requirement, regarding the pressure drop, as

$$p'_f - p_f = \{(1 - \epsilon)/\epsilon\} \dot{w}_n.$$

Hence the boundary conditions appropriate for the interface between two different saturated poroelastic media are

$$\begin{aligned} \text{(i)} \quad T'_{zz} &= T_{zz}, & \text{(ii)} \quad T'_{zx} &= T_{zx}, & \text{(iii)} \quad p'_f - p_f &= \{(1 - \epsilon)/\epsilon\} \dot{w}_z, \\ \text{(iv)} \quad u'_x &= u_x, & \text{(v)} \quad u'_z &= u_z, & \text{(vi)} \quad w'_z &= w_z, \end{aligned} \tag{11}$$

(quantities with prime correspond to the medium M').

REFLECTION AND REFRACTION

We consider only two-dimensional problems in the x - z plane. The incident wave is assumed to originate in medium M and become incident at the interface $z = 0$, making an

angle θ with the z -axis. It results in three reflected waves (P_1 , P_2 and SV) in medium M and three waves (P_1 , P_2 and SV) transmitted to medium M' , as shown in Fig. 1.

From eqns (8), displacement potentials for reflected waves are written as:

$$\phi_j = A_j \exp \{i\delta_j(x \sin \theta_j - z \cos \theta_j) - i\Omega t\}; \quad (j = 1, 2, 3), \quad (12)$$

where $\phi_j = (-\Psi_j)_j$ and arbitrary constants A_1 , A_2 , A_3 denote the amplitudes of reflected P_1 , P_2 and SV waves respectively.

Similarly the corresponding potentials for waves transmitted to medium M' are written as

$$\phi'_j = B_j \exp \{i\delta'_j(x \sin \theta'_j + z \cos \theta'_j) - i\Omega t\}, \quad (j = 1, 2, 3), \quad (13)$$

with the corresponding quantities defined for the medium M' .

Displacement potentials for the incident wave are as follows:

(i) for incident P_1 wave

$$\phi_1 = A_0 \exp \{i\delta_1(x \sin \theta_0 + z \cos \theta_0) - i\Omega t\}, \quad \phi_2 = 0, \quad \phi_3 = 0, \quad (14a)$$

(ii) for incident P_2 wave

$$\phi_1 = 0, \quad \phi_2 = A_0 \exp \{i\delta_2(x \sin \theta_0 + z \cos \theta_0) - i\Omega t\}, \quad \phi_3 = 0, \quad (14b)$$

(iii) for incident SV wave

$$\phi_1 = 0, \quad \phi_2 = 0, \quad \phi_3 = A_0 \exp \{i\delta_3(x \sin \theta_0 + z \cos \theta_0) - i\Omega t\}. \quad (14c)$$

Corresponding to the potentials given by (12)-(14), the boundary conditions (11) are satisfied for all values of x if and only if

$$(i) \quad \delta_j \sin \theta_j = \delta_0 \sin \theta_0 = \delta'_j \sin \theta'_j, \quad (j = 1, 2, 3), \quad (15)$$

where $\delta_0 = \delta_j$ ($j = 1, 2, 3$), as the incident wave is P_1 , P_2 and SV respectively.

$$(ii) \quad \sum_{i=1}^6 a_{ij} Z_i = b_j, \quad (i = 1, 2, \dots, 6), \quad (16)$$

where $Z_1 = B_1/A_0$, $Z_2 = B_2/A_0$, $Z_3 = B_3/A_0$, $Z_4 = A_1/A_0$, $Z_5 = A_2/A_0$ and $Z_6 = A_3/A_0$ represent the amplitude ratios for refracted P_1 , P_2 , SV and reflected P_1 , P_2 and SV waves respectively.

The coefficients a_{ij} in eqns (16) are as follows:

$$\begin{aligned} a_{11} &= T'_1, \quad a_{12} = T'_2, \quad a_{13} = \mu' \delta_3'^2 \sin 2\theta'_3, \quad a_{14} = -T_1, \quad a_{15} = -T_2, \quad a_{16} = \mu \delta_3^2 \sin 2\theta_3, \\ a_{21} &= \mu' \delta_1'^2 \sin 2\theta'_1, \quad a_{22} = \mu' \delta_2'^2 \sin 2\theta'_2, \quad a_{23} = \mu' \delta_3'^2 \cos 2\theta'_3, \\ a_{24} &= \mu \delta_1^2 \sin 2\theta_1, \quad a_{25} = \mu \delta_2^2 \sin 2\theta_2, \quad a_{26} = \mu \delta_3^2 \cos 2\theta_3, \\ a_{31} &= M'(\alpha' + \mu'_1) \delta_1'^2 \varepsilon, \quad a_{32} = M'(\alpha' + \mu'_2) \delta_2'^2 \varepsilon, \\ a_{33} &= 0, \quad a_{34} = (1 - \varepsilon) \Omega \delta_1 \mu \cos \theta_1 - M(\alpha + \mu_1) \delta_1^2 \varepsilon, \\ a_{35} &= (1 - \varepsilon) \Omega \delta_2 \mu \cos \theta_2 - M(\alpha + \mu_2) \delta_2^2 \varepsilon, \quad a_{36} = (1 - \varepsilon) \Omega \delta_3 \alpha_0 \sin \theta_3, \\ a_{41} &= \delta_1' \sin \theta'_1, \quad a_{42} = \delta_2' \sin \theta'_2, \quad a_{43} = \delta_3' \cos \theta'_3, \\ a_{44} &= -\delta_1 \sin \theta_1, \quad a_{45} = -\delta_2 \sin \theta_2, \quad a_{46} = \delta_3 \cos \theta_3, \\ a_{51} &= \delta_1' \cos \theta'_1, \quad a_{52} = \delta_2' \cos \theta'_2, \quad a_{53} = -\delta_3' \sin \theta'_3, \end{aligned}$$

$$\begin{aligned}
 a_{54} &= \delta_1 \cos \theta_1, & a_{55} &= \delta_2 \cos \theta_2, & a_{56} &= \delta_3 \sin \theta_3, \\
 a_{61} &= \mu'_1 \delta'_1 \cos \theta'_1, & a_{62} &= \mu'_2 \delta'_2 \cos \theta'_2, & a_{63} &= -\alpha'_0 \delta'_3 \sin \theta'_3, \\
 a_{64} &= \mu_1 \delta_1 \cos \theta_1, & a_{65} &= \mu_2 \delta_2 \cos \theta_2, & a_{66} &= \alpha_0 \delta_3 \sin \theta_3
 \end{aligned}
 \tag{17}$$

where

$$T_j = \{2\mu \sin^2 \theta_j - (H + \alpha M \mu_j)\} \delta_j^2, \quad T'_j = \{2\mu' \sin^2 \theta'_j - (H' + \alpha' M' \mu'_j)\} \delta_j'^2, \quad (j = 1, 2).$$

(18)

The constant terms b_i on the right side of eqns (16) are given by

(i) for incident P_r wave

$$\begin{aligned}
 b_1 &= -a_{14}, & b_2 &= a_{24}, & b_3 &= M(\alpha + \mu_1) \delta_1^2 \varepsilon + (1 - \varepsilon) \Omega \delta_1 \mu_1 \cos \theta_1, \\
 b_4 &= -a_{44}, & b_5 &= a_{54}, & b_6 &= a_{64};
 \end{aligned}
 \tag{19a}$$

(ii) for incident P_t wave

$$\begin{aligned}
 b_1 &= -a_{15}, & b_2 &= a_{25}, & b_3 &= M(\alpha + \mu_2) \delta_2^2 \varepsilon + (1 - \varepsilon) \Omega \delta_2 \mu_2 \cos \theta_2, \\
 b_4 &= -a_{45}, & b_5 &= a_{55}, & b_6 &= a_{65};
 \end{aligned}
 \tag{19b}$$

(iii) for incident SV wave

$$b_1 = a_{16}, \quad b_2 = -a_{26}, \quad b_3 = -a_{36}, \quad b_4 = a_{46}, \quad b_5 = -a_{56}, \quad b_6 = -a_{66}.$$

(19c)

We now consider the distribution of energy between different reflected and transmitted waves at the surface element of unit area. Following Achenbach (1973), the scalar product of surface traction and particle velocity per unit area, denoted P^* , represents the rate at which the energy is communicated per unit area of the surface. If the outer normal on the surface element is \hat{n} , we have

$$P^* = T_{rm} n_m \dot{u}_r$$

(20)

where T_{rm} is stress tensor, n_m are direction cosines of unit normal \hat{n} and \dot{u}_r are components of particle velocity.

The time average of P^* over a period, denoted by $\langle P^* \rangle$, represents the average energy transmission per unit surface area per unit time. For fluid-saturated porous medium, taking into account the energy communicated to the fluid portion, we have the rate of energy transmission at $z = 0$, given by

$$P^* = T_{zz} \partial u_z / \partial t + T_{zx} \partial u_x / \partial t + (-p_f) \partial w_z / \partial t.$$

(21)

With the help of the expression $\langle R(f) \cdot R(g) \rangle = \frac{1}{2} R(f \cdot \bar{g})$, for any two complex functions f and g , we obtain the energy ratios giving the rate of average energy transmission of all the transmitted and reflected waves to that of incident wave. These energy ratios, E_i ($i = 1, 2, \dots, 6$), for refracted P_r , P_t , SV ; reflected P_r , P_t and SV waves respectively, are expressed as

$$E_i = \langle P_i^* \rangle / \langle P_0^* \rangle, \quad (i = 1, 2, \dots, 6),$$

(22)

where

$$\begin{aligned}
 \langle P_1^* \rangle &= \{ \lambda' + 2\mu' + M'(x' + \mu_1')^2 \} |Z_1|^2 \text{Real}(\cos \theta_1') / v_1'^3 \\
 \langle P_2^* \rangle &= \{ \lambda' + 2\mu' + M'(x' + \mu_2')^2 \} |Z_2|^2 \text{Real}(\cos \theta_2') / v_2'^3 \\
 \langle P_3^* \rangle &= (\mu' / v_3'^3) |Z_3|^2 \text{Real}(\cos \theta_3') \\
 \langle P_4^* \rangle &= \{ \lambda + 2\mu + M(x + \mu_1)^2 \} |Z_4|^2 \text{Real}(\cos \theta_1) / v_1^3 \\
 \langle P_5^* \rangle &= \{ \lambda + 2\mu + M(x + \mu_2)^2 \} |Z_5|^2 \text{Real}(\cos \theta_2) / v_2^3 \\
 \langle P_6^* \rangle &= (\mu / v_3^3) |Z_6|^2 \text{Real}(\cos \theta_3)
 \end{aligned} \tag{23}$$

and

(i) for incident P_1 wave

$$\langle P_0^* \rangle = \{ \lambda + 2\mu + M(x + \mu_1)^2 \} \cos \theta_0 / v_1^3 \tag{24a}$$

(ii) for incident P_2 wave

$$\langle P_0^* \rangle = \{ \lambda + 2\mu + M(x + \mu_2)^2 \} \cos \theta_0 / v_2^3 \tag{24b}$$

(iii) for incident SV wave

$$\langle P_0^* \rangle = (\mu / v_3^3) \cos \theta_0. \tag{24c}$$

Generalisation

All the expressions involving m derived in the preceding sections are applicable only to non-dissipative poroelastic solids. Taking into account the viscosity of the interstitial fluid, these expressions can be made applicable to a general saturated poroelastic solid by replacing Biot's parameter ' m ' by $(m - i\eta/\Omega\chi)$. χ is permeability and η denotes the viscosity of the interstitial fluid. For higher frequencies, where the Poiseuille flow breaks down, a correction factor is applied to viscosity η , replacing it by ηF . F is a complex function of frequency Ω and is evaluated following Biot (1956a).

NUMERICAL RESULTS AND DISCUSSION

Since a large number of parameters enter into the final expressions, in order to study the dependence of amplitude and energy ratios on the angle of incidence of incident wave as well as pore alignment parameter, we confine our numerical work to a particular model. We may mention here that the aim of this study is to discuss the effects of pore alignment on the reflection and refraction. Therefore, for the sake of simplicity, poroelastic solid is assumed to be a non-dissipative one.

Keeping in mind the availability of numerical data, we consider the model consisting of water-saturated sandstone in welded contact with water-saturated limestone. Following the experimental results given by Yew and Jogi (1976) and earlier data given by Fatt (1959), we choose the following values of relevant parameters:

(i) for water-saturated sandstone (medium M)

$$\begin{aligned}
 \lambda &= 0.3034 \times 10^{11} \text{ dyne cm}^{-2}, & \rho &= 2.17 \text{ g cm}^{-3}, \\
 \mu &= 0.922 \times 10^{11} \text{ dyne cm}^{-2}, & \rho_r &= 1.00 \text{ g cm}^{-3}, \\
 M &= 0.887 \times 10^{11} \text{ dyne cm}^{-2}, & m &= 3.731 \text{ g cm}^{-3}, \\
 \alpha &= 0.3227, & \beta &= 0.268.
 \end{aligned}$$

(ii) for water-saturated limestone (medium M')

$$\begin{aligned} \lambda' &= 1.444 \times 10^{11} \text{ dyne cm}^{-2}, & \rho' &= 2.24 \text{ g cm}^{-3}, \\ \mu' &= 1.209 \times 10^{11} \text{ dyne cm}^{-2}, & \rho'_r &= 1.00 \text{ g cm}^{-3}, \\ M' &= 1.591 \times 10^{11} \text{ dyne cm}^{-2}, & m' &= 6.944 \text{ g cm}^{-3}, \\ \alpha' &= 0.262, & \beta' &= 0.144. \end{aligned}$$

Corresponding to the above given values of parameters, the system of eqns (16) is solved for Z_i by Gauss elimination method using a computer program in FORTRAN-77. For fixed values of ϵ between 0 and 1, the angle of incidence is considered to be varying from normal incidence ($\theta_0 = 0$) to grazing incidence ($\theta_0 = 90^\circ$). Amplitude ratios Z_i are found to depend upon the angle of incidence. The energy ratios are then calculated numerically using the relations (22)–(24).

(i) For incident P_r wave

Amplitude and energy ratios for all the reflected waves decrease with the increase of ϵ except for the reflected P_r wave, which shows a reverse behaviour as the angle of incidence increases to nearly 50° (critical angle for refracted P_r wave). Amplitude and energy ratios increase with the increase of ϵ for refracted P_r and refracted SV waves. However, for refracted P_r wave these ratios decrease with the increase of ϵ . At grazing incidence ϵ has no effect (cf. Figs 2–7).

(ii) For incident P_i wave

Amplitude and energy ratios decrease with the increase of ϵ for all the reflected and refracted waves except for the refracted P_i wave, where these ratios increase. At grazing incidence ϵ has no effect on amplitude and energy ratios (cf. Figs 8–13).

(iii) For incident SV wave

Pore alignment has no effect on reflection and transmission at the normal and grazing incidence. Amplitude and energy ratios for refracted P_r wave decrease with the increase of ϵ except for amplitude showing the reverse behaviour as the angle of incidence increases to nearly 40° (critical angle for reflected P_r wave). Increase of ϵ decreases the amplitude and energy ratios for reflected and refracted P_r waves. For refracted SV wave these ratios increase with ϵ , but for reflected SV wave decrease with the increase of ϵ , up to angle of incidence of incident wave smaller than nearly 67° (critical angle for refracted SV wave) (cf. Figs 14–19).

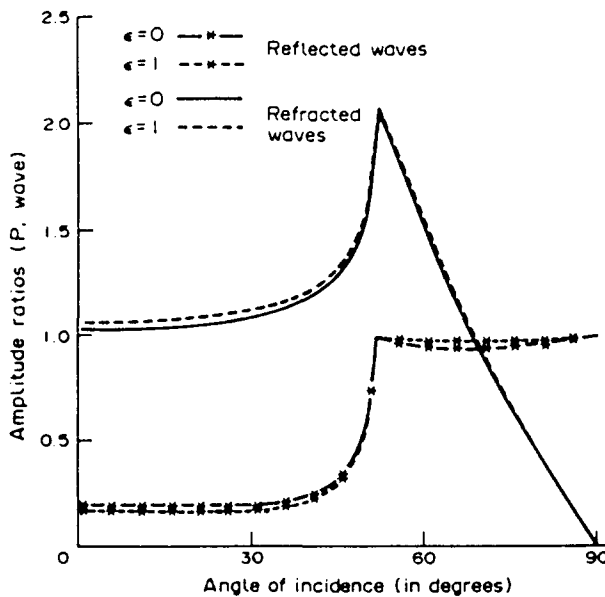


Fig. 2. Amplitude ratios for the reflected and refracted P_r waves for incident P_r wave.

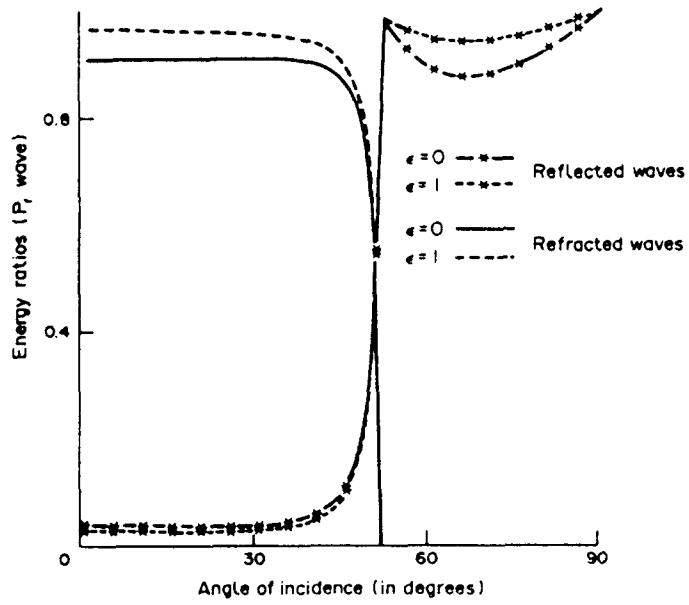


Fig. 3. Energy ratios for the reflected and refracted P_1 waves for incident P_1 wave.

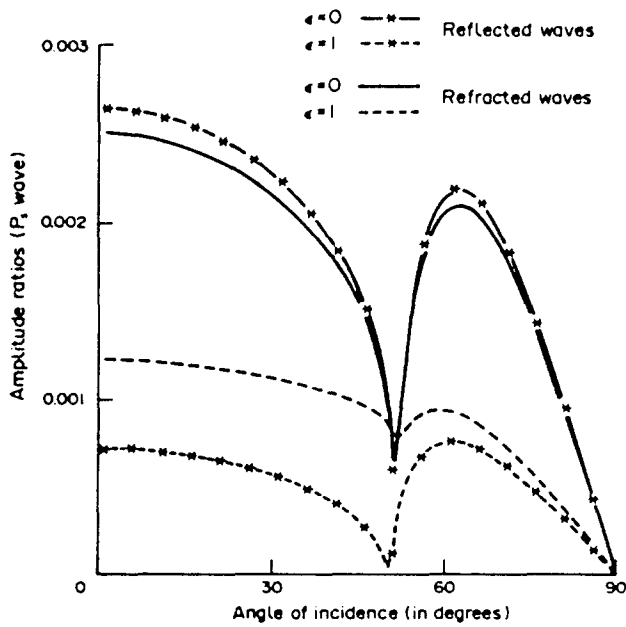


Fig. 4. Amplitude ratios for the reflected and refracted P_1 waves for incident P_1 wave.

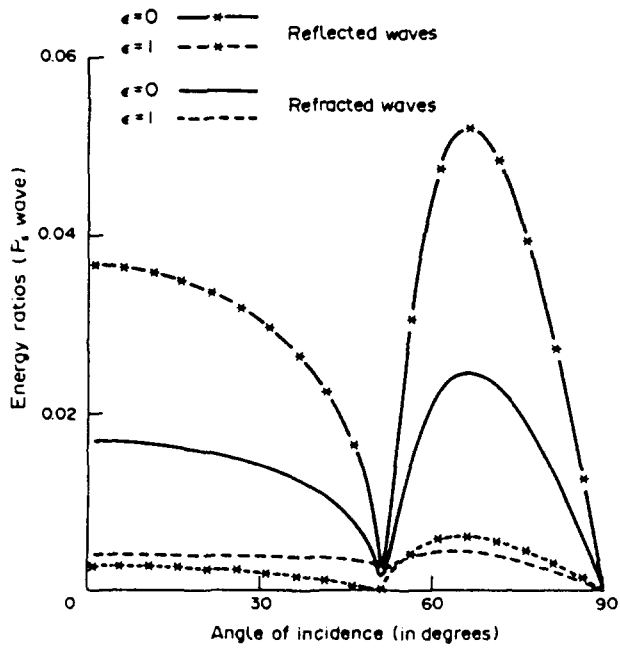


Fig. 5. Energy ratios for the reflected and refracted P_1 waves for incident P_1 wave.

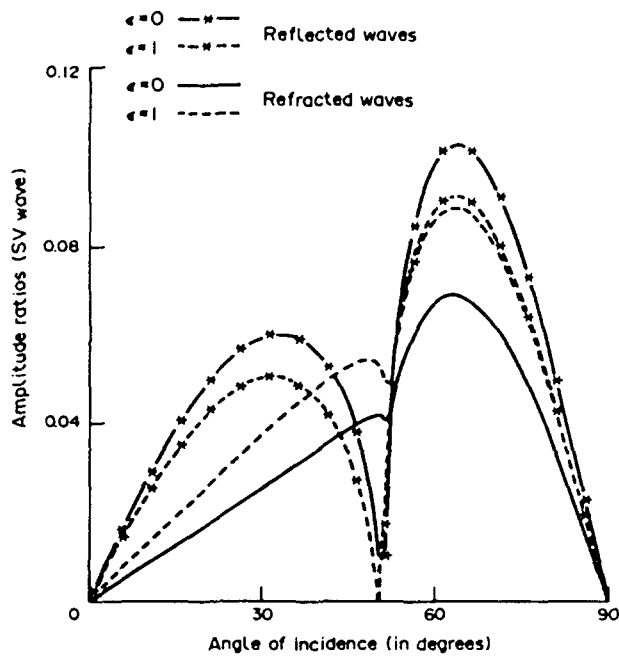


Fig. 6. Amplitude ratios for the reflected and refracted SV waves for incident P_r wave.

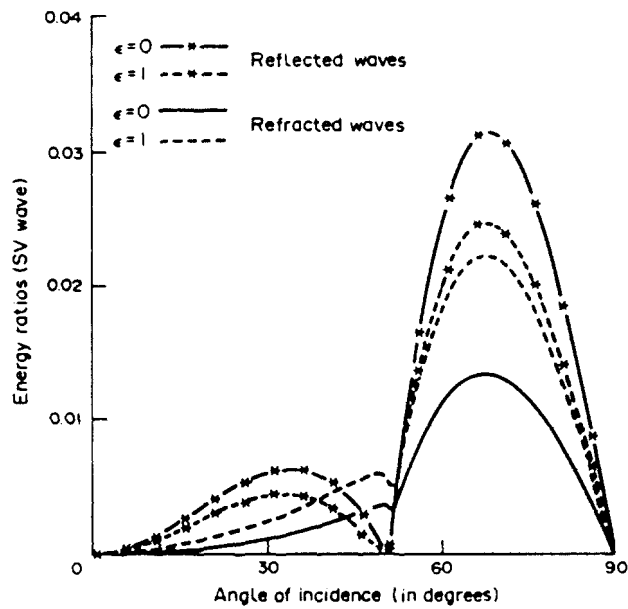


Fig. 7. Energy ratios for the reflected and refracted SV waves for incident P_r wave.

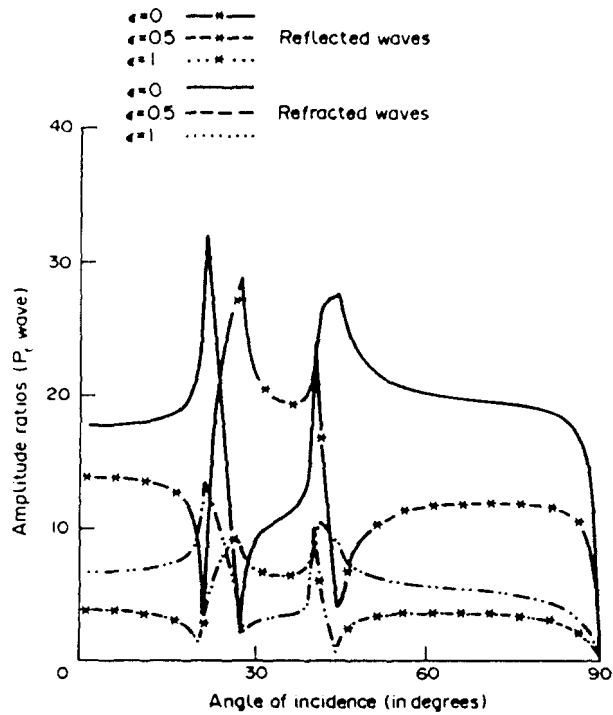


Fig. 8. Amplitude ratios for the reflected and refracted P_r waves for incident P_r wave.

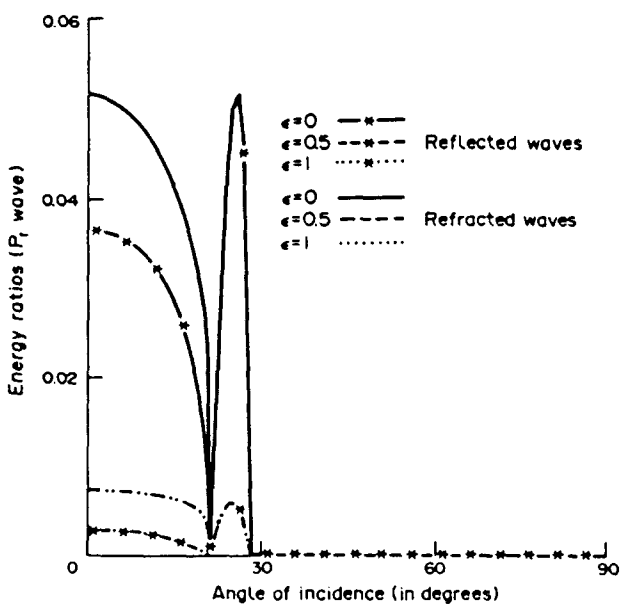


Fig. 9. Energy ratios for the reflected and refracted P_r waves for incident P_i wave.

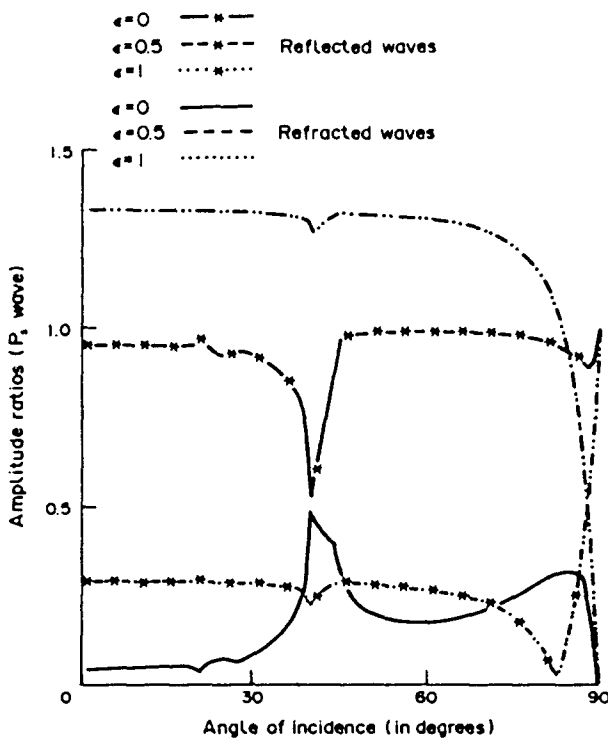


Fig. 10. Amplitude ratios for the reflected and refracted P_r waves for incident P_i wave.

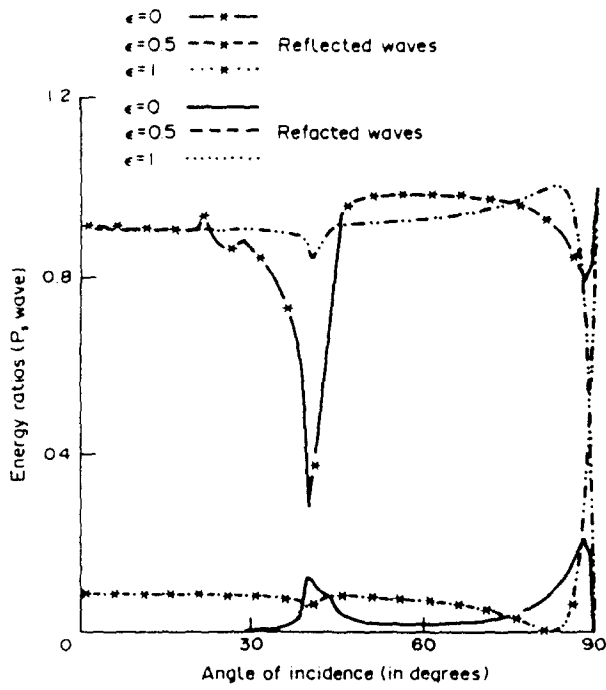


Fig. 11. Energy ratios for the reflected and refracted P₁ waves for incident P₁ wave.

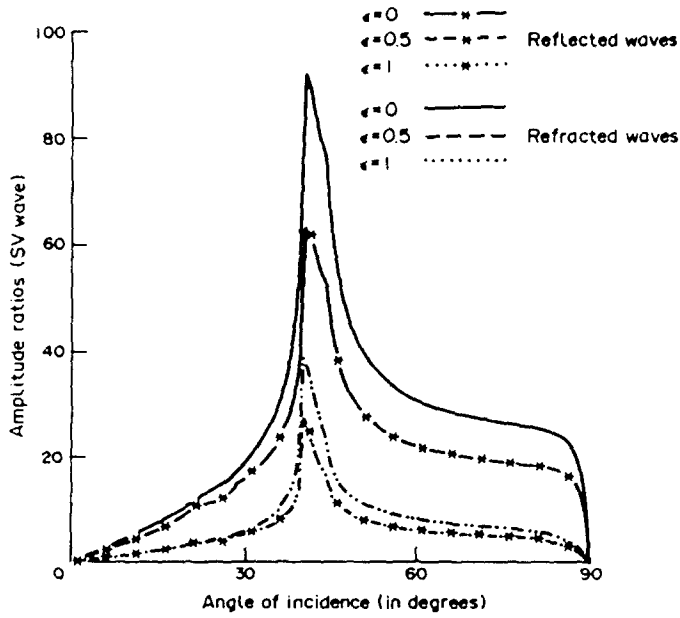


Fig. 12. Amplitude ratios for the reflected and refracted SV waves for incident P₁ wave.

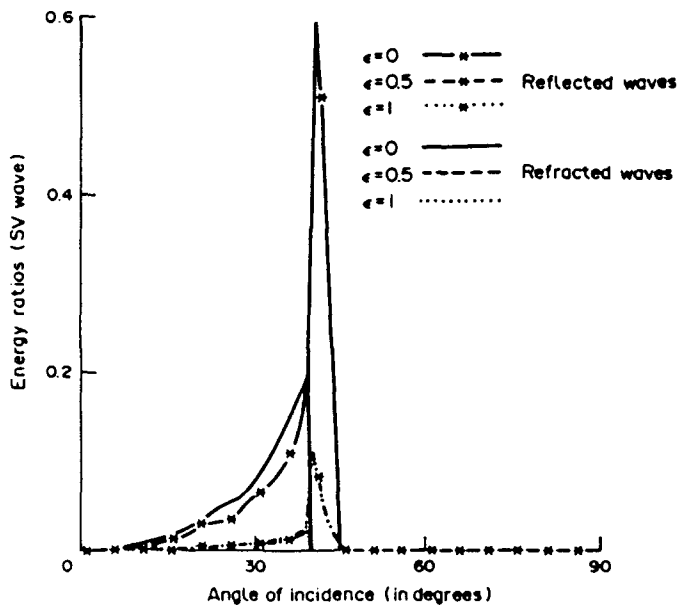


Fig. 13. Energy ratios for the reflected and refracted SV waves for incident P_i wave.

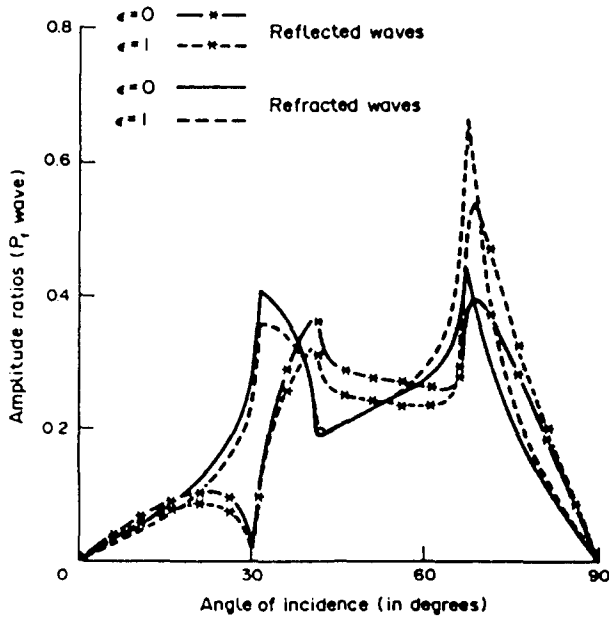


Fig. 14. Amplitude ratios for the reflected and refracted P_r waves for incident SV wave.

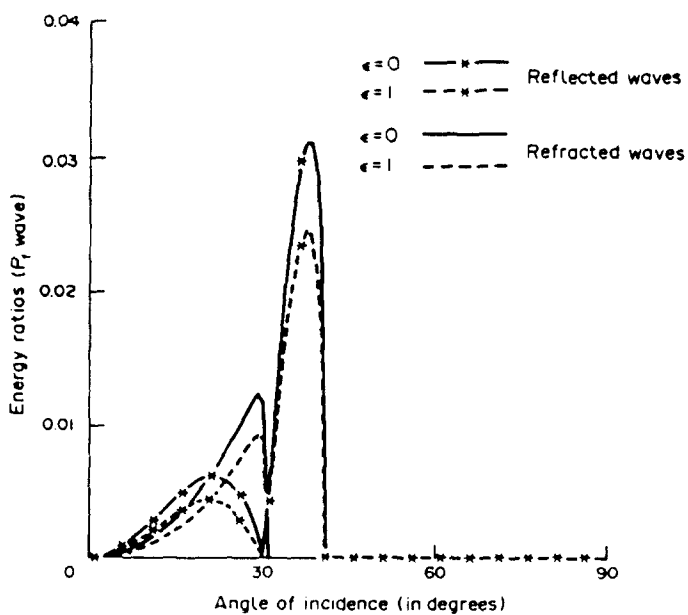


Fig. 15. Energy ratios for the reflected and refracted P_1 waves for incident SV wave.

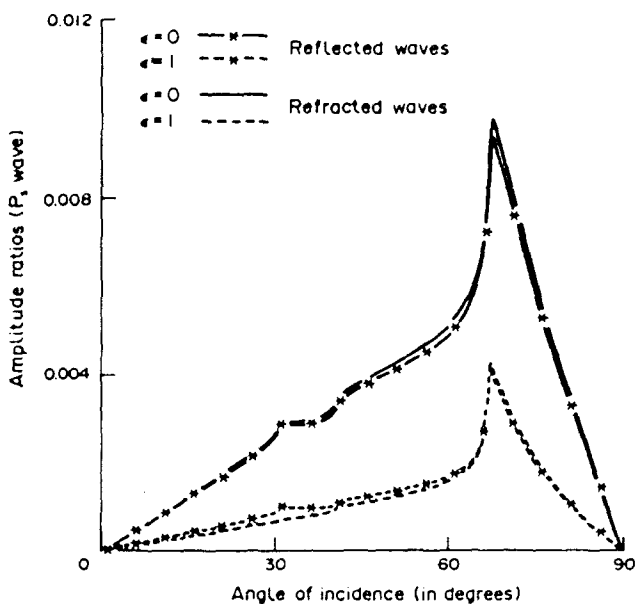


Fig. 16. Amplitude ratios for the reflected and refracted P_1 waves for incident SV wave.

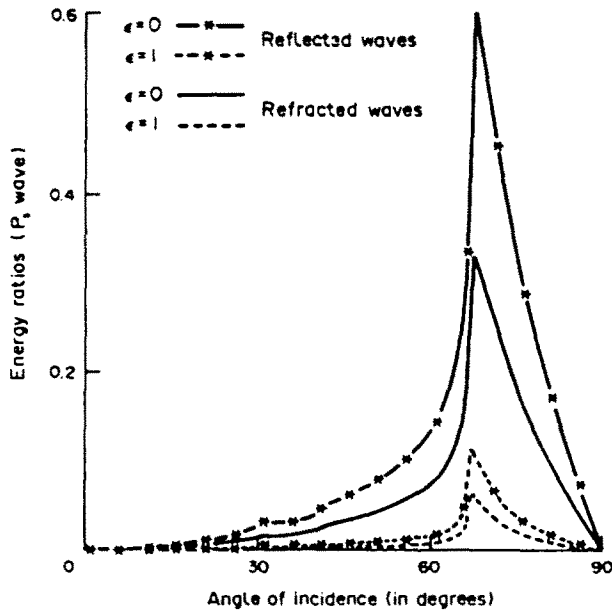


Fig. 17. Energy ratios for the reflected and refracted P_i waves for incident SV wave.

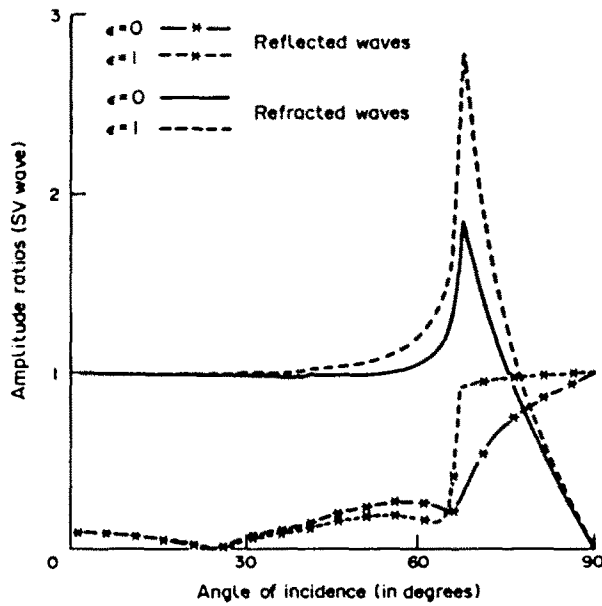


Fig. 18. Amplitude ratios for the reflected and refracted SV waves for incident SV wave.

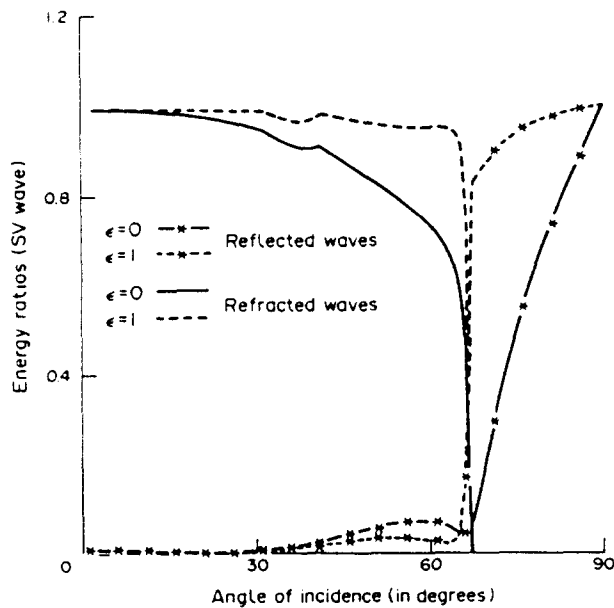


Fig. 19. Energy ratios for the reflected and refracted SV waves for incident SV wave.

It is concluded that pore alignment has no effect at grazing incidence for all the waves. Also it does not affect the normal incidence of SV waves. It is observed that amplitude and energy ratios change infinitesimally with the change in the value of ϵ , except when ϵ is very near to zero. It shows that it does not matter whether the pores at the interface of two media are fully connected or partially connected. It is in accordance with the change in pressure drop for nonalignment of a portion of pores. It can also be checked from equations (16) that the value of ϵ does not affect the entries a_i significantly, except when ϵ tends to zero. Graphs plotted for the extreme values of ϵ show a considerable effect of connection of pores at the interface on amplitude and energy ratios of reflected and refracted waves.

From the numerical results we see that at $z = 0$ $\sum_{i=1}^n E_i = 1$, for each angle of incidence of every incident wave. This implies that no energy is dissipated during transmission at the interface.

It is hoped that this work may be useful in studies, both theoretical and observational, of fault mechanism in the porous solids present in the earth. It may also be helpful in the further studies of wave propagation at the porous/porous interface.

Acknowledgements—The authors are thankful to Professor M. L. Gogna, Department of Mathematics, Kurukshetra University, for providing the computation facilities. The first author is obliged to the Council of Scientific and Industrial Research, DELHI, for providing the financial assistance in the form of Research Associateship.

REFERENCES

- Achenbach, J. D. (1973). *Wave Propagation in Elastic Solids*. North-Holland, Amsterdam.
- Biot, M. A. (1956a). The theory of propagation of elastic waves in a fluid-saturated porous solid. *J. Acoust. Soc. Am.* **28**, 168–191.
- Biot, M. A. (1956b). General solution of the equations of elasticity and consolidation for a porous material. *J. Appl. Mech.* **23**, 91–95.
- Biot, M. A. (1962). Mechanics of deformation and acoustic propagation in porous media. *J. Appl. Phys.* **33**, 1482–1498.
- Burridge, R. and Vargas, C. A. (1979). The fundamental solutions in dynamic poroelasticity. *Geophys. J. R. Astro. Soc.* **58**, 61–90.
- Deresiewicz, H. and Rice, J. T. (1962). The effect of boundaries on wave propagation in a liquid-filled porous solid—III. Reflection of plane waves at free plane boundary. *Bull. Seism. Soc. Am.* **52**, 595–625.
- Deresiewicz, H. and Skalak, R. (1963). On uniqueness in dynamic poroelasticity. *Bull. Seism. Soc. Am.* **53**, 783–789.
- Fatt, I. (1959). Biot-Willis elastic coefficients for a sandstone. *J. Appl. Mech.* **26**, 296–297.
- Hajra, S. and Mukhopadhyay, A. (1982). Reflection and refraction of seismic waves incident obliquely at the boundary of liquid saturated porous solid. *Bull. Seism. Soc. Am.* **72**, 1509–1533.

- Sharma, M. D. and Gogna, M. L. (1991). Seismic waves in viscoelastic porous solid saturated by viscous liquid. *PAGEOPH* (in press).
- Sharma, M. D., Kumar, R. and Gogna, M. L. (1990a). Surface wave propagation in a transversely isotropic elastic layer overlying a liquid saturated porous solid half space and lying under a uniform layer of liquid. *PAGEOPH* **133**, 523-540.
- Sharma, M. D., Kumar, R. and Gogna, M. L. (1990b). Surface wave propagation in a liquid saturated porous layer overlying a homogeneous transversely isotropic half space and lying under a uniform layer of liquid. *Int. J. Solids Structures* **27**(10), 1255-1268.
- Yew, C. H. and Jogi, P. N. (1976). Study of wave motions in fluid-saturated porous rocks. *J. Acoust. Soc. Am.* **60**, 2-8.
- Yew, C. H. and Wang, X. (1987). A study of reflection and refraction of waves at the interface of water and porous sea ice. *J. Acoust. Soc. Am.* **82**, 342-353.